

BMB Reports – Manuscript Submission

Manuscript Draft

**Manuscript Number:** BMB-20-136

**Title:** Combined application of rapamycin and atorvastatin improves lipid metabolism in apolipoprotein E-deficient mice with chronic kidney disease

**Article Type:** Article

**Keywords:** Chronic kidney disease; Atherosclerosis; Rapamycin; Atorvastatin; Co-administration

**Corresponding Author:** Goo Taeg Oh

**Authors:** Goo Taeg Oh<sup>1,\*</sup>, Eun Ju Song<sup>1,3,#</sup>, Sanghyun Ahn<sup>2,#</sup>, Seung-Kee Min<sup>2</sup>, Jongwon Ha<sup>2</sup>

**Institution:** <sup>1</sup>Life Sciences, Ewha Womans University,  
<sup>2</sup>Surgery, Seoul National University College of Medicine,  
<sup>3</sup>Veterinary Physiology, Seoul National University College of Veterinary Medicine,

1 **Article**

2 **Combined application of rapamycin and atorvastatin improves lipid metabolism in**  
3 **apolipoprotein E-deficient mice with chronic kidney disease**

4 Eun Ju Song<sup>1,3#</sup>, Sanghyun Ahn<sup>2#</sup>, Seung-Kee Min<sup>2</sup>, Jongwon Ha<sup>2\*</sup>, Goo Taeg Oh<sup>1\*</sup>

5

6 <sup>1</sup>Immune and Vascular Cell Network Research Center, National Creative Initiatives,  
7 Department of Life Sciences, Ewha Womans University

8 <sup>2</sup>Department of Surgery, Seoul National University College of Medicine, Seoul, Korea

9 <sup>3</sup>Department of Veterinary Physiology, BK21 PLUS Program for Creative Veterinary  
10 Science Research, Research Institute for Veterinary Science and College of Veterinary  
11 Medicine, Seoul National University

12

13 **Running Title:** RAPA plus ATV reduces cardiovascular risk in CKD

14 **Keywords:** Chronic kidney disease, Atherosclerosis, Rapamycin, Atorvastatin, Co-  
15 administration

16

17 \*Corresponding authors. Goo Taeg Oh, Tel: +82-2-3277-4128; Fax: +82-2-3277-3760; E-  
18 mail: gootaeg@ewha.ac.kr; Jongwon Ha, Tel: +82-2-2072-2991; Fax: +82-2-766-3971; E-  
19 mail: jwhamd@snu.ac.kr

20

21 \*These authors contributed equally to the work.

**ABSTRACT**

Atherosclerosis arising from the pro-inflammatory conditions associated with chronic kidney disease (CKD) increases major cardiovascular morbidity and mortality. Rapamycin (RAPA) is known to inhibit atherosclerosis under CKD and non-CKD conditions, but it can cause dyslipidemia; thus, the co-application of lipid-lowering agents is recommended. Atorvastatin (ATV) has been widely used to reduce serum lipids levels, but its synergistic effect with RAPA in CKD remains unclear. Here, we analyzed the effect of their combined treatment on atherosclerosis stimulated by CKD in apolipoprotein E-deficient (*ApoE*<sup>-/-</sup>) mice. Oil Red O staining revealed that treatment with RAPA and RAPA+ATV, but not ATV alone, significantly decreased the atherosclerotic lesions in the aorta and aortic sinus, compared to those seen in the control (CKD) group. The co-administration of RAPA and ATV improved the serum lipid profile and raised the expression levels of proteins involved in reverse cholesterol transport (LXR $\alpha$ , CYP7A1, ABCG1, PPAR $\gamma$ , ApoA1) in the liver. The CKD group showed increased levels of various genes encoding atherosclerosis-promoting cytokines in the spleen (*Tnf- $\alpha$* , *Il-6* and *Il-1 $\beta$* ) and aorta (*Tnf- $\alpha$*  and *Il-4*), and these increases were attenuated by RAPA treatment. ATV and RAPA+ATV decreased the levels of *Tnf- $\alpha$*  and *Il-1 $\beta$*  in the spleen, but not in the aorta. Together, these results indicate that, in CKD-induced *ApoE*<sup>-/-</sup> mice, RAPA significantly reduces the development of atherosclerosis by regulating the expression of inflammatory cytokines and the co-application of ATV improves lipid metabolism.

**INTRODUCTION**

Atherosclerosis and arterial calcification are more frequent and severe in patients with chronic kidney disease (CKD) than in the general population (1). Uremia in CKD patients

46 precipitates oxidative stress and inflammation in the arteries and stimulates plaque formation,  
47 in a process that is called accelerated atherosclerosis (2, 3). As a result, CKD patients exhibit  
48 increased morbidity and mortality due to cardiovascular diseases (4).

49 The pathogenic mechanism of atherosclerosis in CKD can be explained by an imbalance  
50 of electrolytes, such as calcium (Ca) and phosphate (P), and a loss of vascular smooth-muscle  
51 cell (VSMC) function (5). Because the kidney is the main organ for cytokine removal, CKD  
52 patients exhibit cytokine dysregulation and persistent inflammation, which can stimulate  
53 vascular cell senescence (6-8). CKD also promotes dyslipidemia; this is an alteration of  
54 cholesterol homeostasis that includes increased low-density lipoprotein cholesterol (LDL-C)  
55 and decreased high-density lipoprotein cholesterol (HDL-C) levels, and is known to  
56 exacerbate atherosclerosis (9).

57 Several studies have reported that rapamycin (RAPA) suppresses the development of  
58 atherosclerosis and arterial calcification (10, 11). However, RAPA also has been associated  
59 with hyperlipidemia in renal transplant recipients and CKD patients, because mTOR  
60 inhibition reduces the plasma lipid clearance by inhibiting the activity of lipases required for  
61 the catabolism of circulating lipoproteins and altering the expression of enzymes for fatty-  
62 acid uptake and storage (12, 13). Thus, it is recommended that lipid-lowering agents be  
63 administered together (14). The statin, atorvastatin (ATV), has been widely used to prevent  
64 major cardiovascular complications associated with hypercholesterolemia and dyslipidemia.  
65 ATV reportedly plays an anti-inflammatory role by inhibiting the production of tumor  
66 necrosis factor (TNF)- $\alpha$  and protecting VSMCs against TGF- $\beta$ 1-mediated stimulation, and  
67 thereby protects against atherogenesis (15, 16). Although ATV shows a protective effect  
68 against cardiovascular disease, its use in CKD patients has been limited to date (17). A  
69 previous study found that ATV significantly reduced total cholesterol levels and LDL-C

70 independent of CKD, and decreased triglyceride levels more in patients with CKD than in  
71 those without CKD (18). However, the potential synergism of RAPA and ATV (RAPA+ATV)  
72 co-treatment has not been studied in terms of atherosclerosis inhibition, especially in CKD.

73 To understand the mechanism of CKD-accelerated atherosclerosis in depth, *in vivo* CKD  
74 models are required. Although several mouse models have been developed for investigating  
75 the mechanisms of atherosclerosis caused by CKD, limitations exist because the genetic  
76 manipulations or inducing methods are associated with various degrees of renal failure (19).  
77 In this study, we established a distinct CKD mouse model promoting atherosclerosis  
78 compared with sham operated mice. And we investigated the effects of RAPA+ATV on the  
79 regulation of inflammatory cytokines and dyslipidemia to prevent the development of  
80 atherosclerosis in CKD-induced apolipoprotein E-deficient (*ApoE*<sup>-/-</sup>) mice.

81

## 82 RESULTS

### 83 *RAPA ameliorates CKD-associated atherosclerosis*

84 To establish a consistent CKD mouse model, we used a two-step surgical nephrectomy in  
85 8-week-old female *ApoE*<sup>-/-</sup> mice (Supplemental Fig. 1A). We first evaluated the serum  
86 chemistry (Table 1) and found that the levels of blood urea nitrogen (BUN), creatinine, and  
87 calcium were markedly increased in the sera of mice subjected to surgical nephrectomy  
88 compared to sera in sham-operated mice. However, RAPA and/or ATV did not decrease the  
89 uremia and the hypercalcemia associated with CKD in mice. No significant between-group  
90 difference was seen in the serum phosphate level.

91 To find out the effect of RAPA and/or ATV on atherosclerotic lesions accelerated by CKD,  
92 we established the CKD mouse model as described above, and the mice were further fed a  
93 Western diet to induce atherosclerosis. This model was used in all subsequent experiments.

94 Oil red O staining showed that the CKD group exhibited more atherosclerotic plaque  
95 formation in the whole aorta than did the Sham group (Fig. 1A). The RAPA and RAPA+ATV  
96 groups exhibited significant reductions of the atherosclerotic lesions, whereas the ATV group  
97 did not differ from the CKD group. There was no significant difference between the RAPA  
98 and RAPA+ATV groups in this parameter. We observed similar results when we analyzed the  
99 stained aortic sinuses of mouse hearts (Fig. 1B). Together, these findings indicate that RAPA  
100 reduces the atherosclerosis associated with CKD in this model, but ATV has no additional  
101 effect on this parameter, alone or in combination with RAPA.

102

### 103 ***Combination of RAPA and ATV improves lipid metabolism in CKD mice***

104 It has been reported that CKD patients may exhibit dyslipidemia, which is a major risk  
105 factor for the development of cardiovascular disease (20). To find the serum lipid levels in  
106 our experimental system, we fasted animals for 4 hours, sacrificed them, and collected whole  
107 blood for serum chemistry. The serum levels of total cholesterol and triglyceride were not  
108 different between the groups (Figs. 2A and 2B). Circulating LDL-C was significantly more  
109 increased in the CKD group than in the Sham and was inhibited in the ATV group. However,  
110 neither RAPA nor RAPA+ATV affected the LDL-C level elevated by CKD in those groups.  
111 The serum level of HDL-C in the CKD and RAPA group was similar to that in the Sham  
112 group, but the level was markedly elevated in the ATV and RAPA+ATV groups (Figs. 2C and  
113 2D). Surprisingly, the HDL-C levels in the co-administration of RAPA and ATV were higher  
114 than that seen in the ATV group, with an increase that was twice those seen in the Sham and  
115 CKD groups. To explore the effect of RAPA and ATV on lipid metabolism, we used qRT-  
116 PCR to evaluate the mRNA expression levels of genes related to cholesterol metabolism,  
117 including *Hmgcr*, *Lxra*, *Abcg5*, *Cyp7a1*, *Ppar $\gamma$* , and *Apoa1*, in the livers of our experimental

118 and control mice (Supplemental Figs. 2A-2F). As expected, CKD increased the mRNA  
119 expression level of *Hmgcr*, and this change was inhibited by treatment with RAPA and/or  
120 ATV. The *Hmgcr* expression level did not differ between the RAPA, ATV, and RAPA+ATV  
121 groups, and the levels of all three groups were lower than that of the sham group. CKD  
122 tended to decrease the gene expression levels of *Lxra* compared to those in the sham group.  
123 The gene expression of *Lxra* was significantly higher in the RAPA and/or ATV groups than in  
124 the CKD and sham groups. The classical pathway of bile acid initiated by *Cyp7a1* was more  
125 inhibited in the CKD group than in the sham group. The RAPA+ATV group had significantly  
126 higher *Cyp7a1* expression than did the CKD group. In addition, combined administration of  
127 RAPA and ATV significantly increased the mRNA level of *Abcg5*, *Pparγ* and *Apoa1*, whereas  
128 this parameter did not differ between the RAPA, ATV, sham, and CKD groups.

129 We subsequently examined the expression level of proteins related to reverse cholesterol  
130 transport, including LXR $\alpha$ , CYP7A1, ABCG1, PPAR $\gamma$ , and ApoA1, in the mouse liver (Figs.  
131 3E and 3F). The CKD group significantly reduced the expression of LXR $\alpha$  to be similar to  
132 that in the Sham group by ATV administration, but the levels were not affected by RAPA  
133 treatment. Interestingly, the RAPA+ATV group had significantly elevated expression levels of  
134 LXR $\alpha$ , CYP7A1, ABCG1 and ApoA1 in the liver. The expression level of PPAR $\gamma$  was  
135 slightly lowered in the CKD group, but there was no significant difference between any of the  
136 groups. Given the results, we found that co-administration of RAPA and ATV is more  
137 effective in stimulating reverse cholesterol transport and bile secretion than is ATV treatment  
138 alone. These data suggest that combining RAPA with ATV may help to mitigate dyslipidemia  
139 in CKD.

140

141 *ApoE<sup>-/-</sup> mice with CKD exhibit up-regulation of pro-inflammatory cytokine genes in the*

142 *spleen and aorta, and these levels are reduced by RAPA*

143 Next, we used qRT-PCR to investigate the effects of RAPA and/or ATV on the expression  
144 levels of atherogenesis-related inflammatory cytokines. In the spleen, the mRNA expression  
145 of inflammatory cytokines is known to promote atherosclerosis, including *Tnf- $\alpha$* , *Il-6*, and *Il-*  
146 *1 $\beta$* , which were specifically more increased in the CKD group than in the sham group (Figs.  
147 4A-4C). The CKD-related up-regulations of *Tnf- $\alpha$*  and *Il-1 $\beta$*  were suppressed in the ATV,  
148 RAPA, and RAPA+ATV groups, and their levels did not significantly differ between these  
149 groups. The administration of RAPA significantly inhibited the CKD-related increase of *Il-6*  
150 expression, whereas this level was similar among the ATV, ATV+RAPA, and CKD groups.  
151 Interestingly, *Il-10*, an anti-inflammatory cytokine, was more increased in the CKD group  
152 than in the sham group, and this increase was suppressed in the ATV and RAPA+ATV groups  
153 (Fig. 4D).

154 In the aorta, the mRNA levels of *Tnf- $\alpha$*  and *Il-4* were higher in the CKD group than in the  
155 sham group (Figs. 4E and 4F), whereas the RAPA group had significantly lower levels of *Tnf-*  
156  *$\alpha$*  and *Il-4* than did the CKD group. However, ATV and RAPA+ATV did not decrease their  
157 levels like RAPA did. Surprisingly, the mRNA expression level of *Il-6* did not differ in any of  
158 the groups (Fig. 4G). The mRNA level of *Il-10* was significantly increased in the RAPA  
159 group over that in the sham and CKD groups (Fig. 4H), but this significant increase was not  
160 seen in the RAPA+ATV group. These results suggest that the administration of RAPA helps  
161 decrease the levels of atherosclerosis-promoting cytokines and increases those of  
162 atherosclerosis-suppressing cytokines, but that combined treatment with RAPA and ATV does  
163 not appear to show these synergistic effects.

164

165 **DISCUSSION**

166 We herein provide the first report on how combined treatment with RAPA and ATV  
167 affects the atherogenesis stimulated by CKD. In our study, the oral administration of RAPA in  
168 CKD-induced *ApoE*<sup>-/-</sup> mice ameliorated atherosclerotic lesions and inhibited the mRNA  
169 expression levels of pro-inflammatory cytokines in the spleen and aorta. These data confirm  
170 that RAPA plays an athero-protective role by reducing the pro-inflammatory burden in CKD.  
171 Although ATV did not additionally reduce the aortic lesions, the combined use of ATV  
172 markedly increased the serum levels of HDL-C in *ApoE*<sup>-/-</sup> mice with CDK. Thus, our results  
173 suggest that the combination therapy of RAPA plus ATV helps to alleviate the atheroprone  
174 environment of CKD.

175 The formation of atherosclerotic lesions can differ with the stage of renal failure. An  
176 electronic cautery-based renal injury mouse model has been used in various CKD studies,  
177 because such mice exhibit substantial increases in their serum levels of BUN and creatinine  
178 (21, 22). However, these methods did not show sufficient or consistent renal impairment in  
179 our preliminary experiments (data not shown). We instead used high-temperature battery-  
180 operated cautery to forcefully damage the kidney and found that this procedure yielded a  
181 consistent CKD model. The serum calcium and phosphate levels of operated mice were  
182 significantly elevated, supporting the idea that our model is suitable for the mechanistic study  
183 of CKD. Since uncontrolled lipid homeostasis promotes atherosclerosis, the ability of the  
184 reverse cholesterol-transport pathway to eliminate excessive serum lipids is an important  
185 factor in reducing the risk of cardiovascular disease (23). Previous study revealed that  
186 experimental chronic uremia increased serum LCL-C and stimulated atherosclerosis in mice  
187 (24). Likewise, we found more LDL-C in the serum of CKD-induced mice than in the Sham.  
188 However, there were no differences in the serum total cholesterol and triglyceride between

189 the two groups. These findings suggest that maintaining the balance of LCL-C and HDL-C is  
190 important for improving atherosclerosis in CKD.

191 RAPA has been shown to significantly suppress atherosclerosis in studies using animal  
192 models with normal renal function (10, 11), but there are still concerns about adverse effects  
193 that may be associated with RAPA treatment, such as dyslipidemia. In our results,  
194 atherosclerotic lesions were substantially reduced by RAPA administration in CKD mice, but  
195 the serum lipids levels were not influenced. Several studies have reported that mTOR  
196 inhibition limits the serum lipid elimination by suppressing lipase activity and cholesterol  
197 trafficking (12, 13, 25, 26). It was also reported that RAPA treatment increases circulating  
198 PCSK9 levels, which are related to the increased serum LDL-C and hypercholesterolemia in  
199 patients with nephrotic syndrome (27, 28). These findings support the limitation of RAPA use  
200 in CKD patients. Further study will be needed to elucidate the role of RAPA in PCSK9-  
201 associated dyslipidemia. Several researchers suggested that combined treatment with a statin  
202 would reduce the possibility of RAPA-induced dyslipidemia, resulting in additional  
203 amelioration of atherosclerosis (29, 30). This prompted us to examine the potential of ATV to  
204 counter this disadvantage of RAPA treatment. Consistent with previous findings, our results  
205 showed that the decreased expression of LXR $\alpha$  and CYP7A1 in the liver of CKD mice was  
206 compensated by ATV administration. LXR $\alpha$  has long been suggested as a therapeutic target  
207 against atherosclerosis, since it is implicated in cholesterol efflux and hepatic bile-acid  
208 synthesis by regulating the expression of target genes associated with reverse cholesterol  
209 transport, including CYP7A1, ABCG1/5/8 and apolipoproteins (31, 32). Meanwhile, LXR $\alpha$   
210 increases fatty-acid (FA) and triglyceride (TG) synthesis by upregulating genes, including  
211 SREBPc, FA synthase, and acetyl coenzyme A carboxylase (33). However, accumulated work  
212 has clearly shown the beneficial effect of LXR $\alpha$  agonist against atherosclerosis. Furthermore,

213 our study demonstrated that CKD mice treated with RAPA plus ATV gained weight  
214 (Supplementary Fig. 1B) and exhibited stabilization of the HDL-C level (Fig. 2C). The  
215 combined use of RAPA and ATV further promoted the expression of ABCG1 and ApoA1,  
216 which contribute more to cholesterol efflux than does RAPA or ATV alone. Given that  
217 hepatic ApoA1 synthesis decreases and HDL-C level falls are common effects of renal failure  
218 (34), our study suggests that the activation of LXR $\alpha$ /ApoA1/ABCG1 by RAPA and ATV co-  
219 administration improves the stability of HDL-C and atherosclerosis in CKD (35). These  
220 results suggest that the combined treatment could be synergistic in eliminating the excessive  
221 serum lipids promoting atherosclerosis, and improving general conditions and long-term  
222 mortality in mice with renal failure.

223 Dysregulation of cytokines in CKD is associated with a significant decrease in cytokine  
224 secretion, given that the kidney is a main organ for eliminating cytokines (9). RAPA was  
225 previously shown to target pro-inflammatory cytokines and mTOR activation induced by  
226 chronic consumption of a high-fat diet (36). Indeed, we found that RAPA, ATV, and  
227 RAPA+ATV all markedly decreased the gene expression levels of atherosclerosis-promoting  
228 inflammatory cytokines such as *Tnf- $\alpha$* , *Il-6* and *Il-1 $\beta$*  in the spleen. Interestingly, the mRNA  
229 level of the anti-inflammatory cytokine, *Il-10*, was increased in the spleen tissues of the CKD  
230 group. This appears to be a compensatory mechanism intended to correct inflammation in  
231 CKD (38). In the aorta, RAPA specifically decreased the level of *Il-4* and increased the level  
232 of *Il-10*, indicating that it exerts anti-inflammatory effects to prevent atherogenesis.  
233 Conversely, these levels were similar in the ATV, RAPA+ATV, and CKD groups. Several  
234 reports have suggested that ATV can have inhibitory effects on atherosclerosis in non-CKD  
235 models (39, 40). Thus, the previous and present results demonstrate that RAPA and ATV can  
236 both regulate the systemic inflammation environment in CKD patients, but that these effects

237 are not synergistic.

238 In conclusion, we herein show that RAPA can play a critical role in reducing the  
239 development of atherosclerosis in the aortas of CKD-induced *ApoE*<sup>-/-</sup> mice by alleviating  
240 systemic inflammation. Although the co-administration of ATV did not further reduce  
241 atherosclerosis, it improved the lipid profile and bile-acid metabolism in these mice. Thus,  
242 the combined administration of RAPA and ATV can provide synergistic effects in alleviating  
243 the cardiovascular risk associated with CKD, beyond the effects of either agent alone.

244

#### 245 **MATERIALS AND METHODS**

246 The detailed methods are described in the “Supplementary Information”.

247

#### 248 **ACKNOWLEDGMENTS**

249 This study was supported by the Research Resettlement Fund for the new faculty of Seoul  
250 National University, a grant from the SNUH Research Fund (04-2016-0360), and a grant  
251 from the National Research Foundation of Korea (NRF) funded by the Korean government  
252 (NRF-2012R1A3A2026454). The funders and company had no role in study design, data  
253 collection, analysis, the decision to publish, or preparation of the manuscript.

254

#### 255 **CONFLICTS OF INTEREST**

256 The authors declare no conflicts of interest.

257

258 **FIGURE LEGENDS**

259 Table 1. Body weight and laboratory data of *ApoE*<sup>-/-</sup> mice with CKD at the end of the  
260 study

261 Figure 1. RAPA ameliorates the formation of atherosclerotic plaques, as assessed by Oil  
262 red O staining. (A) Representative *en face* images of whole aortas (left) and quantification of  
263 lesion areas from the indicated groups (right) (*ApoE*<sup>-/-</sup>; *n* = 6-7 per group). (B) Representative  
264 images of frozen sections of aortic sinuses (left) and quantification of plaque areas on aortic  
265 sinuses of the indicated groups (right) (*n* = 3-5 per group). Data are shown as mean ± SEM,  
266 \**p* < 0.05, \*\**p* < 0.01 compared with the sham group; #*p* < 0.05, ##*p* < 0.01 compared with the  
267 CKD group.

268 Figure 2. Combined treatment with RAPA plus ATV has beneficial effects on lipid  
269 metabolism. Serum lipid profiles for (A) total cholesterol, (B) triglycerides, (C) low-density  
270 lipoprotein cholesterol (LDL-C), and (D) high-density lipoprotein cholesterol (HDL-C) from  
271 the indicated groups (*n* = 6-9). (E, F) The expression levels of reverse cholesterol transport-  
272 related proteins in the livers of the indicated groups (*n* = 5 per group). Data are shown as  
273 mean ± SEM, \**p* < 0.05, \*\**p* < 0.01 compared with the sham group; #*p* < 0.05, ##*p* < 0.01  
274 compared with the CKD group.

275 Figure 3. The effects of RAPA and ATV on the CKD-related stimulation of pro-  
276 atherosclerosis cytokines in *ApoE*<sup>-/-</sup> mice. Gene expression levels of inflammatory cytokines  
277 in the spleen (A-D) and aorta (E-H) (*n* = 5-7 per group). Data are shown as mean ± SEM, \**p*  
278 < 0.05, \*\**p* < 0.01 compared with the sham group; #*p* < 0.05, ##*p* < 0.01 compared with the  
279 CKD group.

280

281

## 282 REFERENCES

- 283 1. London GM and Drueke TB (1997) Atherosclerosis and arteriosclerosis in chronic  
284 renal failure. *Kidney Int* 51, 1678-1695
- 285 2. Zoccali C and London G (2015) Con: vascular calcification is a surrogate marker, but  
286 not the cause of ongoing vascular disease, and it is not a treatment target in chronic  
287 kidney disease. *Nephrol Dial Transplant* 30, 352-357
- 288 3. Himmelfarb J, Stenvinkel P, Ikizler TA and Hakim RM (2002) The elephant in uremia:  
289 oxidant stress as a unifying concept of cardiovascular disease in uremia. *Kidney Int*  
290 62, 1524-1538
- 291 4. Ketteler M, Schlieper G and Floege J (2006) Calcification and cardiovascular health:  
292 new insights into an old phenomenon. *Hypertension* 47, 1027-1034
- 293 5. Finch JL, Lee DH, Liapis H et al (2013) Phosphate restriction significantly reduces  
294 mortality in uremic rats with established vascular calcification. *Kidney Int* 84, 1145-  
295 1153
- 296 6. Carrero JJ, Yilmaz MI, Lindholm B and Stenvinkel P (2008) Cytokine dysregulation  
297 in chronic kidney disease: how can we treat it? *Blood Purif* 26, 291-299
- 298 7. Tbahriti HF, Meknassi D, Moussaoui R et al (2013) Inflammatory status in chronic  
299 renal failure: The role of homocysteinemia and pro-inflammatory cytokines. *World J*  
300 *Nephrol* 2, 31-37
- 301 8. Gisterå A and Hansson GK (2017) The immunology of atherosclerosis. *Nat Rev*  
302 *Nephrol* 13, 368-380
- 303 9. Zewinger S, Kleber ME, Rohrer L et al (2017) Symmetric dimethylarginine, high-  
304 density lipoproteins and cardiovascular disease. *Eur Heart J* 38, 1597-1607
- 305 10. Kurdi A, De Meyer GR and Martinet W (2016) Potential therapeutic effects of mTOR

- 306 inhibition in atherosclerosis. *Br J Clin Pharmacol* 82, 1267-1279
- 307 11. Ai D, Jiang H, Westerterp M et al (2014) Disruption of mammalian target of  
308 rapamycin complex 1 in macrophages decreases chemokine gene expression and  
309 atherosclerosis. *Circ Res* 114, 1576-1584
- 310 12. Hoogeveen RC, Ballantyne CM, Pownall HJ et al (2001) Effect of sirolimus on the  
311 metabolism of ApoB100-containing lipoproteins in renal transplant patients.  
312 *Transplantation* 72(7), 1244-1250
- 313 13. Pallet N and Legendre C (2012) Adverse events associated with mTOR inhibitors.  
314 *Expert Opin Drug Saf* 12, 177-186
- 315 14. Kurdi A, Martinet W and De Meyer GRY (2018) mTOR Inhibition and  
316 Cardiovascular Diseases: Dyslipidemia and Atherosclerosis. *Transplantation* 102,  
317 S44-s46
- 318 15. Zhang X, Tian F, Kawai H et al (2012) Anti-inflammatory effect of amlodipine plus  
319 atorvastatin treatment on carotid atherosclerosis in Zucker metabolic syndrome rats.  
320 *Transl Stroke Res* 3, 435-441
- 321 16. Liu D, Cui W, Liu B et al (2014) Atorvastatin protects vascular smooth muscle cells  
322 from TGF- $\beta$ 1-stimulated calcification by inducing autophagy via suppression of the  $\beta$ -  
323 catenin pathway. *Cell Physiol Biochem* 33, 129-141
- 324 17. Koren MJ, Davidson MH, Wilson DJ, Fayyad RS, Zuckerman A and Reed DP (2009)  
325 Focused atorvastatin therapy in managed-care patients with coronary heart disease  
326 and CKD. *Am J Kidney Dis* 53, 741-750
- 327 18. Manni G, Gargaro M, Turco A et al (2018) Statins regulates inflammatory  
328 macrophage phenotype through the activation of AhR. *J Immunol* 200, 167.19-.19
- 329 19. Yang HC, Zuo Y and Fogo AB (2010) Models of chronic kidney disease. *Drug Discov*

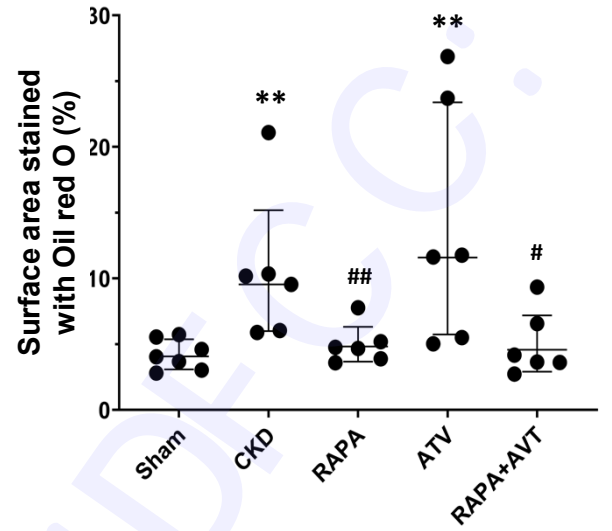
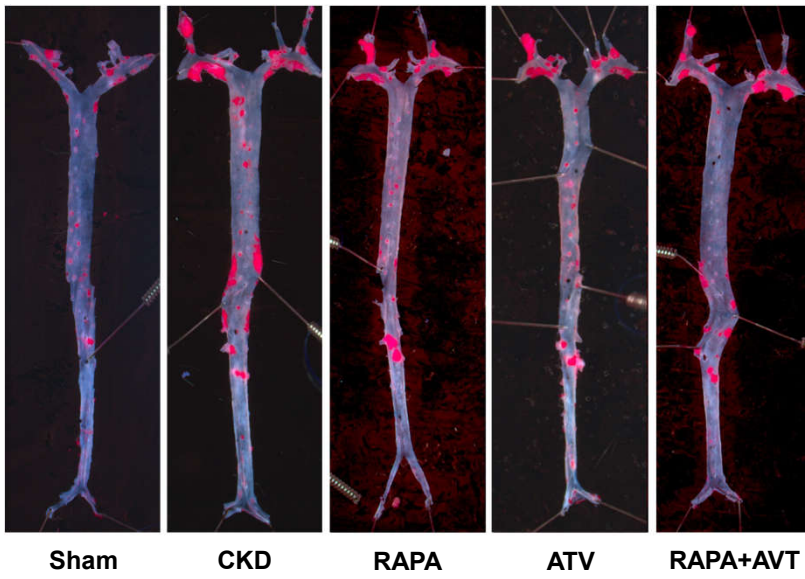
- 330 Today Dis Models 7(1-2), 13–19.
- 331 20. Mikolasevic I, Žutelija M, Mavrinac V and Orlic L (2017) Dyslipidemia in patients  
332 with chronic kidney disease: etiology and management. *Int J Nephrol Renovasc Dis*  
333 10, 35-45
- 334 21. Massy ZA, Ivanovski O, Nguyen-Khoa T et al (2005) Uremia accelerates both  
335 atherosclerosis and arterial calcification in apolipoprotein E knockout mice. *J Am Soc*  
336 *Nephrol* 16, 109-116
- 337 22. Gagnon RF and Gallimore B (1988) Characterization of a mouse model of chronic  
338 uremia. *Urol Res* 16, 119-126
- 339 23. Annema W and Tietge UJ (2012) Regulation of reverse cholesterol transport - a  
340 comprehensive appraisal of available animal studies. *Nutr Metab (Lond)* 9, 25
- 341 24. Apostolov EO, Ray D, Savenka AV, Shah SV and Basnakian AG (2010) Chronic  
342 uremia stimulates LDL carbamylation and atherosclerosis. *J Am Soc Nephrol* 21(11),  
343 1852-1857
- 344 25. Houd VP, Brûlé S, Festuccia WT et al (2010) Chronic rapamycin treatment causes  
345 glucose intolerance and hyperlipidemia by upregulating hepatic gluconeogenesis and  
346 impairing lipid deposition in adipose tissue. *Diabetes* 59(6), 1338-1348
- 347 26. Eid W, Dauner K, Courtney KC et al (2017) mTORC1 activates SREBP-2 by  
348 suppressing cholesterol trafficking to lysosome in mammalian cells. *Proc Natl Acad*  
349 *Sci* 114(30), 7999-8004
- 350 27. Simha V, Qin S, Shah P et al (2017) Sirolimus therapy is associated with elevation in  
351 circulating PCSK9 levels in cardiac transplant patients. *J Cardiovasc Trans Res* 10, 9-  
352 15
- 353 28. Haas ME, Levenson AE, Sun X et al (2016) The role of proprotein convertase

- 354 subtilisin/kexin type 9 in nephrotic syndrome-associated hypercholesterolemia.  
355 *Circulation* 134(1), 61-72
- 356 29. Peng N, Meng N, Wang S et al (2014) An activator of mTOR inhibits oxLDL-induced  
357 autophagy and apoptosis in vascular endothelial cells and restricts atherosclerosis in  
358 apolipoprotein E<sup>-/-</sup> mice. *Sci Rep* 4, 5519
- 359 30. Martinet W, De Loof H and De Meyer GRY (2014) mTOR inhibition: a promising  
360 strategy for stabilization of atherosclerotic plaques. *Atherosclerosis* 233, 601-607
- 361 31. Gupta S, Pandak WM and Hylemon PB (2002) LXR $\alpha$  is the dominant regulator of  
362 CYP7A1 transcription. *Biochem Biophys Res Commun* 293, 338-343
- 363 32. Calkin AC and Tontonoz P (2010) Liver X receptor signaling pathways and  
364 atherosclerosis. *Arterioscler Thromb Vasc Biol* 30(8), 1513-1518
- 365 33. Chisholm JW, Hong J, Mills SA and Lawn RM (2003) The LXR ligand T0901317  
366 induces severe lipogenesis in the db/db diabetic mouse. *J Lipid Res* 44, 2039-2048
- 367 34. Schiffrin EL, Lipman ML and Mann JF (2007) Chronic Kidney Disease. *Circulation*  
368 116, 85-97
- 369 35. Kennedy MA, Barrera GC, Nakamura K et al (2005) ABCG1 has a critical role in  
370 mediating cholesterol efflux to HDL and preventing cellular lipid accumulation. *Cell*  
371 *Metabolism* 1(2), 121-131
- 372 36. Song M, Ahn JH, Kim H et al (2018) Chronic high-fat diet-induced obesity in gerbils  
373 increases pro-inflammatory cytokines and mTOR activation, and elicits neuronal  
374 death in the striatum following brief transient ischemia. *Neurochem Int* 121, 75-85
- 375 37. Soltani A, Bahreyni A, Boroumand N et al (2018) Therapeutic potency of mTOR  
376 signaling pharmacological inhibitors in the treatment of proinflammatory diseases,  
377 current status, and perspectives. *J Cell Physiol* 233, 4783-4790

- 378 38. Stenvinkel P, Ketteler M, Johnson RJ et al (2005) IL-10, IL-6, and TNF-alpha: central  
379 factors in the altered cytokine network of uremia--the good, the bad, and the ugly.  
380 Kidney Int 67, 1216-1233
- 381 39. Zhao X, Liu Y, Zhong Y et al (2015) Atorvastatin Improves Inflammatory Response  
382 in Atherosclerosis by Upregulating the Expression of GARP. Mediators Inflamm 2015,  
383 841472
- 384 40. Li H, Tao HR, Hu T et al (2010) Atorvastatin reduces calcification in rat arteries and  
385 vascular smooth muscle cells. Basic Clin Pharmacol Toxicol 107, 798-802  
386

Figure 1

A



B

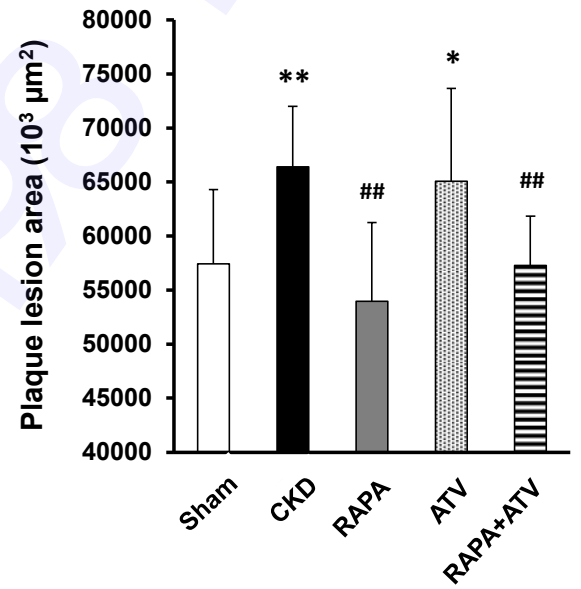
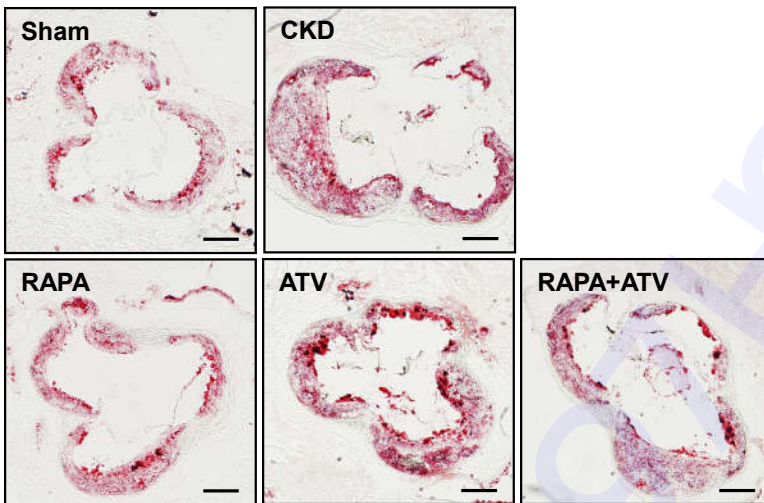


Figure 2

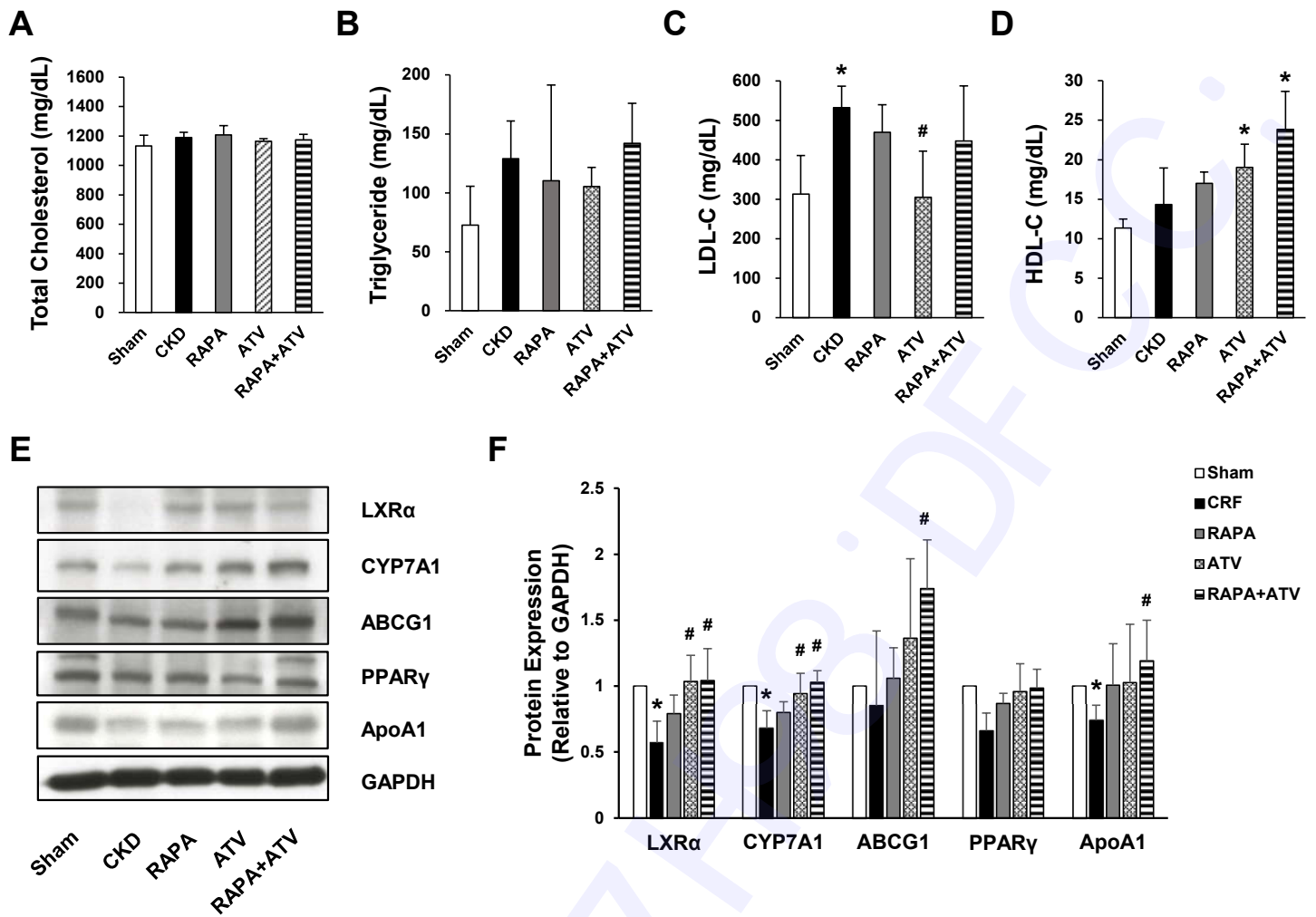
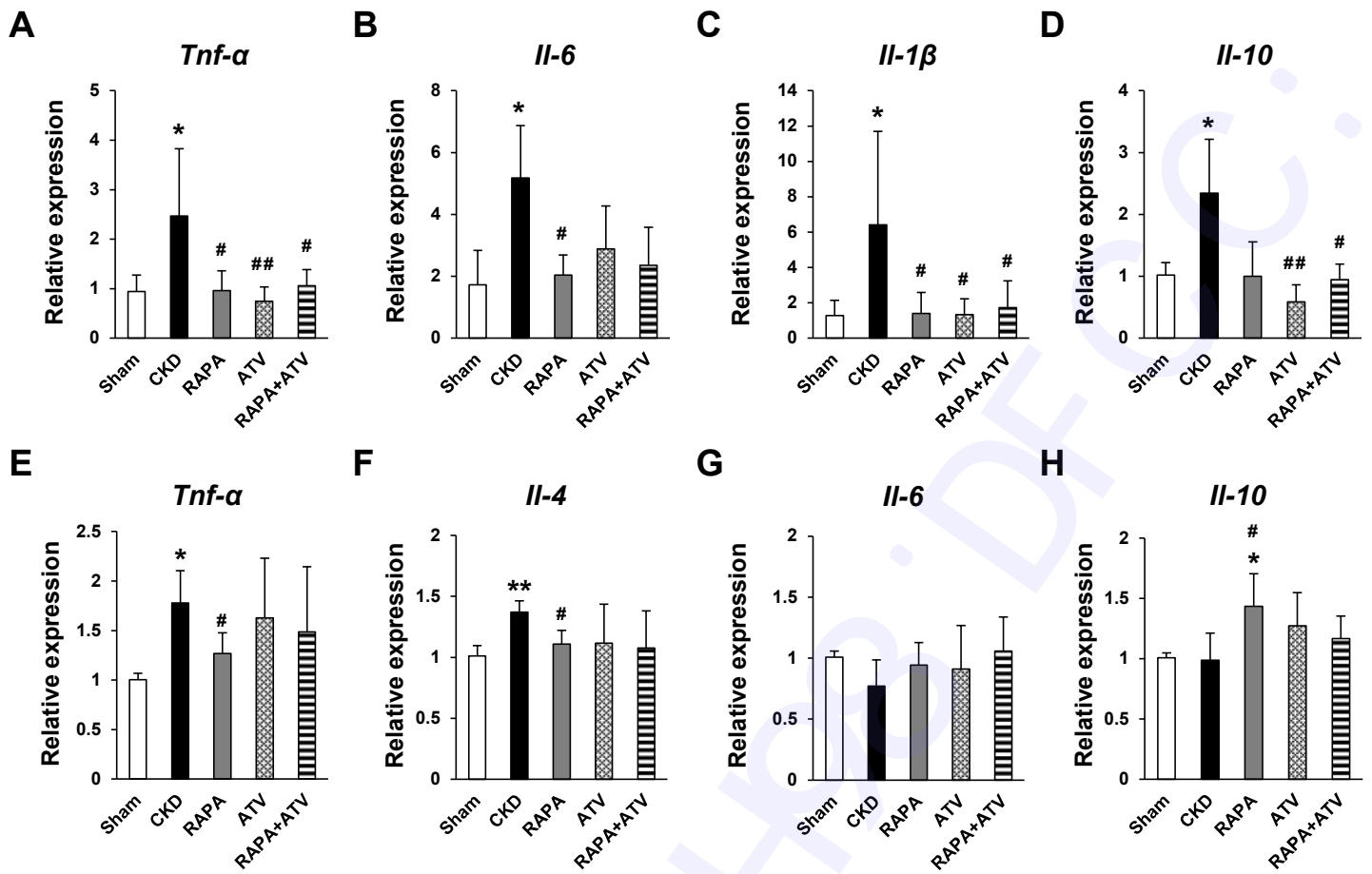


Figure 3



**Table 1. Body weight and laboratory data of *ApoE*<sup>-/-</sup> mice with CKD at the end of the study**

	Sham	CKD	RAPA	ATV	RAPA+ATV
Body weight (g)	22.9 ± 1.2	*20.4 ± 2.4	*20.3 ± 3.0	*20.1 ± 4.1	#22.7 ± 1.5
BUN, mg/dL	18.7 ± 3.9	*92.8 ± 14.4	*78.9 ± 32.8	*79.5 ± 19.5	*65.8 ± 25.2
Creatinine, mg/dL	0.28 ± 0.02	*0.47 ± 0.03	*0.65 ± 0.13	*0.59 ± 0.19	*0.56 ± 0.14
B/C ratio	44.4 ± 39.8	*195.3 ± 19.2	*111.8 ± 28.9	*128.8 ± 24.3	*151.3 ± 23.3
Calcium, mg/dL	9.78 ± 0.39	*11.27 ± 1.48	*10.10 ± 0.67	*10.17 ± 0.7	*11.08 ± 0.42
Phosphate, mg/dL	7.23 ± 0.79	8.0 ± 2.0	6.57 ± 1.78	6.73 ± 1.08	8.72 ± 1
Total protein, g/dL	6.13 ± 1.4	8.27 ± 3.33	7.94 ± 2.86	4.45 ± 0.31	9.21 ± 4.76
Albumin, g/dL	1.67 ± 0.21	1.77 ± 0.4	1.81 ± 0.39	1.28 ± 0.05	1.99 ± 0.62

BUN, blood urea nitrogen; B/C, BUN/Creatinine; AST, aspartate aminotransferase; ALT, alanine aminotransferase; ALP, alkaline phosphatase. Data are shown as mean ± SEM, \**P* < 0.05, \*\**P* < 0.01 compared with Sham group, #*P* < 0.05, ##*P* < 0.01 compared with CKD group.

## Article

### **Combined application of rapamycin and atorvastatin improves lipid metabolism in apolipoprotein E-deficient mice with chronic kidney disease**

Eun Ju Song<sup>1,3#</sup>, Sanghyun Ahn<sup>2#</sup>, Seung-Kee Min<sup>2</sup>, Jongwon Ha<sup>2\*</sup>, Goo Taeg Oh<sup>1\*</sup>

<sup>1</sup>Immune and Vascular Cell Network Research Center, National Creative Initiatives, Department of Life Sciences, Ewha Womans University

<sup>2</sup>Department of Surgery, Seoul National University College of Medicine, Seoul, Korea

<sup>3</sup>Department of Veterinary Physiology, BK21 PLUS Program for Creative Veterinary Science Research, Research Institute for Veterinary Science and College of Veterinary Medicine, Seoul National University

**Running Title:** RAPA plus ATV reduces cardiovascular risk in CKD

**Keywords:** Chronic kidney disease, Atherosclerosis, Rapamycin, Atorvastatin, Co-administration

\*Corresponding authors. Goo Taeg Oh, Tel: +82-2-3277-4128; Fax: +82-2-3277-3760; E-mail: gootaeg@ewha.ac.kr; Jongwon Ha, Tel: +82-2-2072-2991; Fax: +82-2-766-3971; E-mail: jwhamd@snu.ac.kr

\*These authors contributed equally to the work.

## MATERIALS AND METHODS

### *Experimentally induced CKD mouse model (two-step procedure)*

All animal studies were approved by the Institutional Animal Care and Use Committee of Ewha Womans University (IACUC-18-036). All experiments were carried out on female *ApoE*<sup>-/-</sup> mice at 8 weeks of age. The animals were maintained in a specific pathogen-free facility set on a 12-h light-dark cycle, and were given free access to chow diets and sterilized water. A two-step procedure was used to induce uremia. Briefly, the right kidney was dissected from the adrenal gland and surrounding fat through a 2-cm flank incision; it was then cauterized by Bovie High-Temperature Battery-Operated Cautery (Symmetry Surgical, TN, USA), except for 2 mm around the hilum. Two weeks later, the ureter and renal artery and vein were clipped using a surgical clip and left total nephrectomy was performed through a left flank incision. The sham operation used as a control comprised the decapsulation of both kidneys. After 2 weeks of recovery, the mice were divided into the CKD, RAPA, ATV, and RAPA+ATV groups and fed a Western diet (#D12097B; Research Diets, Inc., NJ, USA) for 10 weeks to induce atherogenesis. Where indicated, rapamycin (RAPA; 0.5 mg/kg) or/and atorvastatin (ATV; 10 mg/kg) were given by oral gavage for 5 days a week for 10 weeks. Rapamycin and atorvastatin were supplied by Pfizer.

### *Blood biochemistry*

Whole blood was drawn through the retro-orbital plexus of each deeply anesthetized mouse using a heparin-treated capillary. Serum was separated by centrifugation at 1,500 g for 15 min and stored at -80 °C until analysis. Serum levels of BUN, creatinine, total cholesterol, triglycerides, high-density lipoprotein cholesterol (HDL-C), and low-density lipoprotein

cholesterol (LDL-C) were measured using a Hitachi 7180 biochemistry autoanalyzer (Hitachi Ltd., Tokyo, Japan). The levels of calcium, phosphate, total protein, and albumin were also measured.

#### *Atherosclerotic lesion analysis*

Mice were euthanized with carbon dioxide inhalation, and the hearts and aortas were perfused through the left ventricle with ice-cold phosphate-buffered saline (PBS). Hearts, including the aortic roots, were embedded in frozen-section compound (3801480; Leica, IL, USA) and serially sectioned at 7  $\mu\text{m}$ . For *en face* analysis, the aorta was opened along the longitudinal axis and pinned onto a black wax plate. For measurement of atherosclerotic plaque lesions, the aorta and the heart section were fixed with 10% formalin in PBS and stained using an Oil red O solution. The lesion areas were analyzed using the Axio Vision software (Carl Zeiss, Jena, Germany).

#### *RNA isolation and quantitative real-time PCR*

Total RNA from tissue samples was prepared with the TRIzol reagent (Gibco, CA, USA), and cDNA was synthesized with the Maxime<sup>TM</sup> RT-PCR PreMix (iNtRON Biotechnology, Korea). Quantitative real-time PCR (SYBR<sup>®</sup> FAST, Kappa Biosystems, MA, USA) was conducted to determine the relative levels of mRNA using a 7700 sequence detector (Applied Biosystems, CA, USA) and primers for the target mouse genes (Supplementry Table 1). The data were normalized to the mRNA level of *Gapdh* in each reaction.

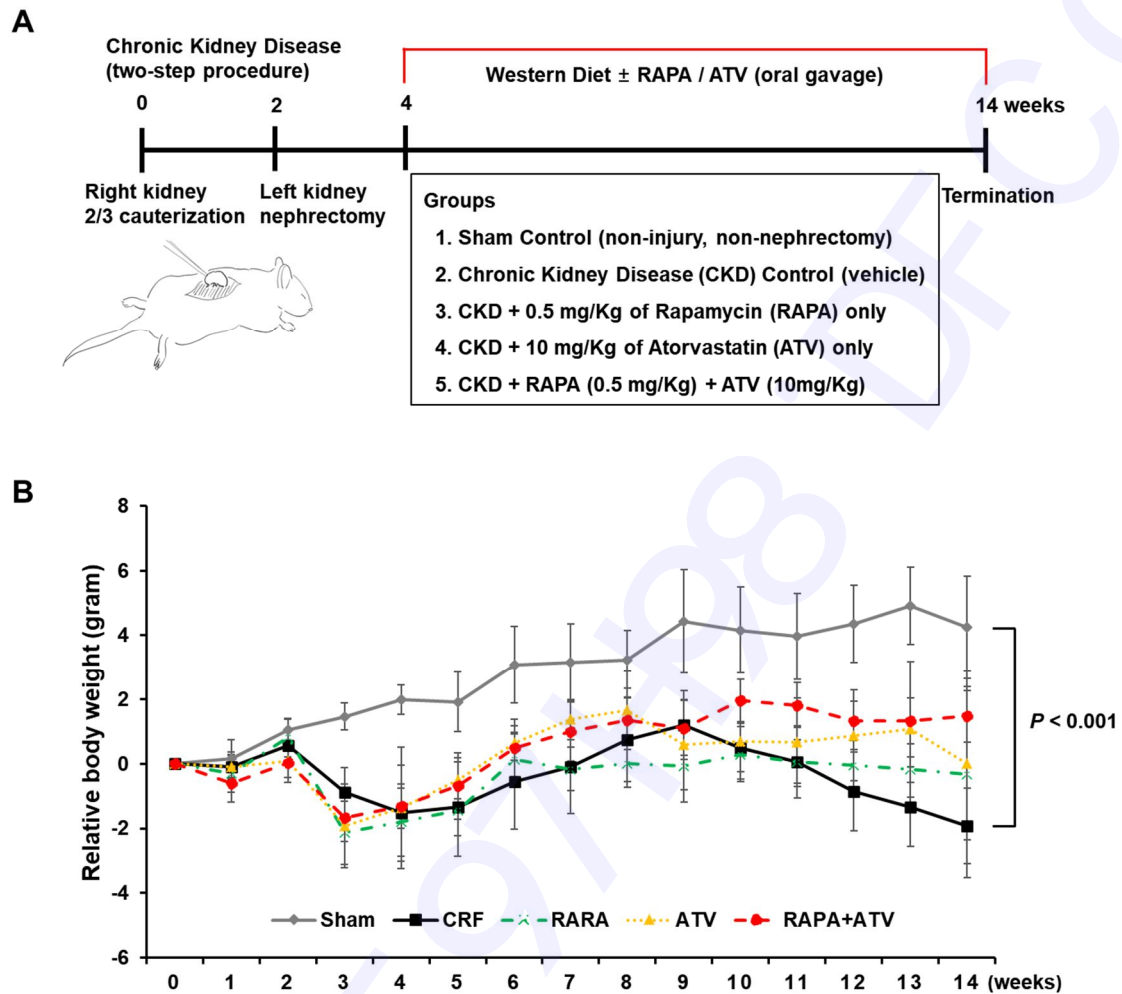
### *Western Blot Analysis*

Total protein was extracted from tissue samples using EzRIPA Lysis buffer containing protease and phosphatase inhibitor cocktail (ATTO, Tokyo, Japan). For analysis of target protein expression, proteins were separated by SDS-PAGE and transferred onto a PVDF membrane. The membrane was incubated in primary antibodies at 4 °C for overnight, and with secondary antibodies for 2 hours at room temperature. Immunoreactive bands were visualized and quantified. Antibodies for target protein were purchased as follows: anti-LXR $\alpha$  (Abcam, Cambridge, UK); anti-Cyp7a1, anti-PPAR $\gamma$ , anti-IL6 and anti-VCAM1 (Santa Cruz Biotechnology, CA, USA); anti-ABCG1 (Novus Biologicals, CO, USA); anti-ApoA1 (Biodesign, ME, USA); anti-GAPDH and HRP-conjugated goat anti-mouse/rabbit IgG antibodies (GeneTex, TX, USA).

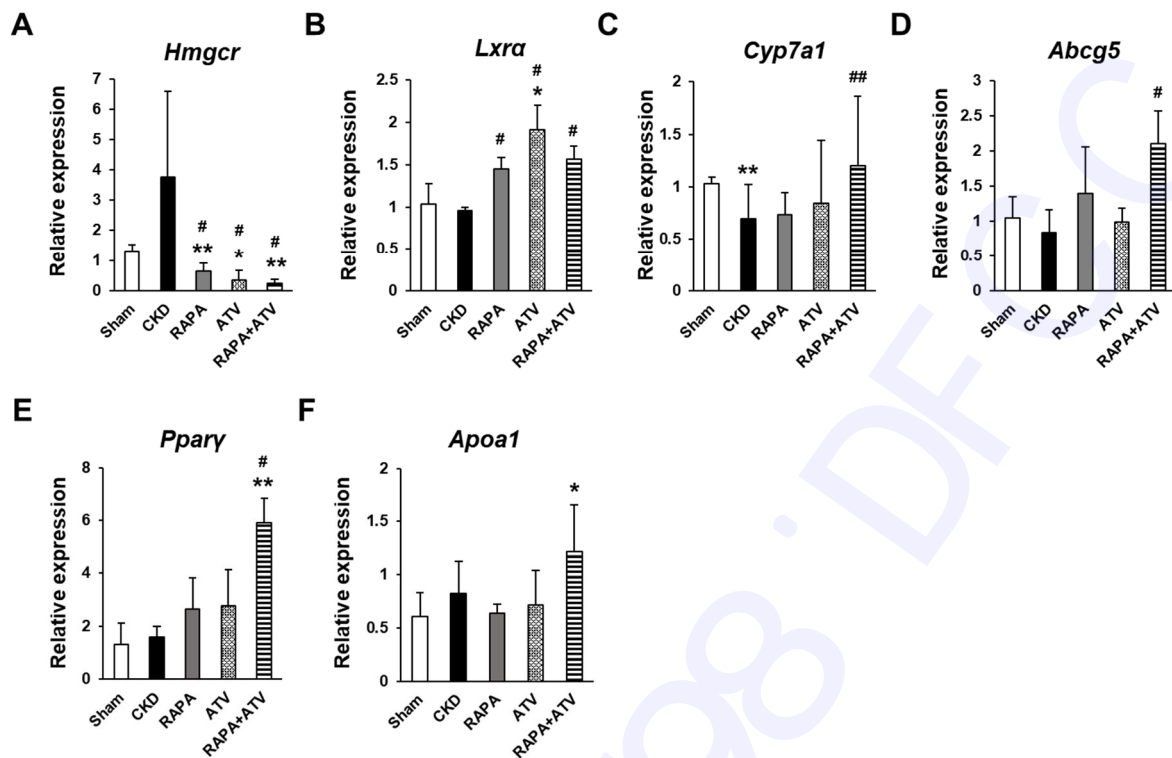
### *Statistical analysis*

Continuous variables are expressed as the mean  $\pm$  standard deviation and were compared using the Mann-Whitney *U* test. Categorical variables were tested with Fisher's exact tests and are expressed as counts and percentages. Body weights were analyzed using a repeated-measures ANOVA followed by Bonferroni's post-hoc test. Analyses were performed with the SPSS Statistical Analytics software (IBM Analytics, NY, USA).

## SUPPLEMENTARY FIGURES



Supplementary Figure 1. (A) Schematic presentation of the experimental protocol. (B) Changes in the body weights of experimental animals.



Supplementary Figure 2. mRNA expression levels of (A) cholesterol metabolism-related genes, (B, C) cholesterol transport-related genes, (D) bile acid biosynthesis genes, and (E, F) lipid and glucose metabolism-related genes in the livers of the indicated groups (n=5-7 per group). Data are shown as mean  $\pm$  SEM, \*P < 0.05, \*\*P < 0.01 compared with the sham group; #P < 0.05, ##P < 0.01 compared with the CKD group.

## SUPPLEMENTARY TABLE

Supplementary Table 1. Primer sequences

Gene	Sequence (5' -> 3')	
	Forward primer	Reverse primer
<i>Hmgcr</i>	TTTCTAGAGCGAGTGCATTAGCA	GATTGCCATTCCACGAGCTATAT-3'
<i>Lxra</i>	GATGTTTCTCCTGATTCTGCAAC	AGGACTTGAGGAGGTGAGGAC
<i>Abcg5</i>	CCTGCTGAGGCGAGTAACAA	TGGCACCCACAAGCTGATAG
<i>Cyp7a1</i>	CACTCTACACCTTGAGGATGG	GACATATTGTAGCTCCTGATCC
<i>Pparγ</i>	AGATTCAGAAGAAGAACCGAAC	CCGATCTCCACAGCAAATTATAG
<i>Apoa1</i>	GCATGCGCACACCGTAGACTCTCT	CGTCTCCAGCATGGGCATCAGACTA
<i>Tnf-α</i>	TGGCCCAGACCCTCACACTCAG	ACCCATCGGCTGGCACCCT
<i>Il-6</i>	CTTCCATCCAGTTGCCTTCTTG	AATTAAGCCTCCGACTTGTGAAG
<i>Il-1β</i>	GGAGAACCAAGCAACACAAAATA	TGGGGA ACTCTGCAGACTCAAAC
<i>Il-10</i>	GCTCTTACTGACTGGCATGAG	CGCAGCTCTAGGAGCATGTG
<i>Il-4</i>	GAATGTACCAGGAGCCATATC	CTCAGTACTACGATGAATCCA
<i>Gapdh</i>	CATCACTGCCACCCAGAAGACTG	ATGCCAGTGAGCTTCCCGTTCAG